

## Behavior of Hydrogen-Terminated Si(111) Surface in Oxygen-Dissolved NH<sub>4</sub>F Solution with or without Cu(II) Ions

Sang-Eun Bae, Jong-Soon Lee, In-Churl Lee, Moon-Bong Song, and Chi-Woo J. Lee\*

Department of Advanced Materials Chemistry, Korea University, Jochiwon, Choongnam 339-700, Korea

\*E-mail: cwlee@korea.ac.kr

Received August 2, 2005

**Key Words :** Si(111), Oxygen, Ammonium fluoride, Cu(II), STM

In the conjunction with the development of ultra-large-scale integration circuits (ULSI), the skill of the control of contaminants in cleansing solutions and also the technology for making a flat hydrogen-terminated Si single crystal surface should be developed in the near future.<sup>1,2</sup> To obtain an ideal hydrogen-terminated Si(111), Higashi *et al.* used a basic solution<sup>3</sup> and Watanabe *et al.* used boiling water<sup>4</sup> as an etching solution. The kind and pH of aqueous electrolyte solutions, miscut angle and orientation of Si(111) wafer, and dissolved oxygen and contaminants in cleansing solution are important factors to consider to get atomically flat terrace on Si(111) surface.

We previously studied the electroless deposition of copper on the hydrogen-terminated Si(111) surface immersed in nitrogen-purged 40% NH<sub>4</sub>F solution containing Cu(II) ions by means of STM and ATR-FTIR.<sup>5</sup> Cu nano particles were found to be deposited on the step edge of the terrace of a hydrogen-terminated Si(111) surface. The hydrogen-terminated Si stretching intensity of 2084 cm<sup>-1</sup> decreased as Cu(II) concentration increased. In this work, we wish to report about the effects of the two common impurities, oxygen and Cu(II), on the preparation of the flat hydrogen-terminated Si(111) surface by wet process.

Figures 1(a) and 1(b) show an ATR-FTIR spectrum of the hydrogen-terminated Si(111) surface with *p*-polarization mode and its STM image obtained under dry nitrogen environments, respectively, after immersing in nitrogen-purged 40% NH<sub>4</sub>F solution for 5 min. A sharp peak at 2084 cm<sup>-1</sup> was observed with an absorbance of 0.13. This peak was attributed to the Si-H stretching mode of the monohydride terminated on the Si(111) surface, characterized by a polarization perpendicular to the surface.<sup>5</sup> Figure 1(a) was used as a reference when the ATR-FTIR peak at 2084 cm<sup>-1</sup> was normalized in the presence of oxygen and/or Cu(II) ions in etching solutions (*vide infra*). The STM image indicated that the hydrogen-terminated Si(111) surface had wide terraces of 50 nm with a step height of about 3 Å. Therefore, it was firmly concluded from both ATR-FTIR and STM results that hydride was mostly bound on the Si(111) terrace as a monohydride.<sup>5,6</sup>

To investigate the effect of a dissolved oxygen, the hydrogen-terminated Si(111) surface was introduced into oxygen-saturated 40% NH<sub>4</sub>F solution for 5 min. Before the measurements the sample was blown-dried by a nitrogen

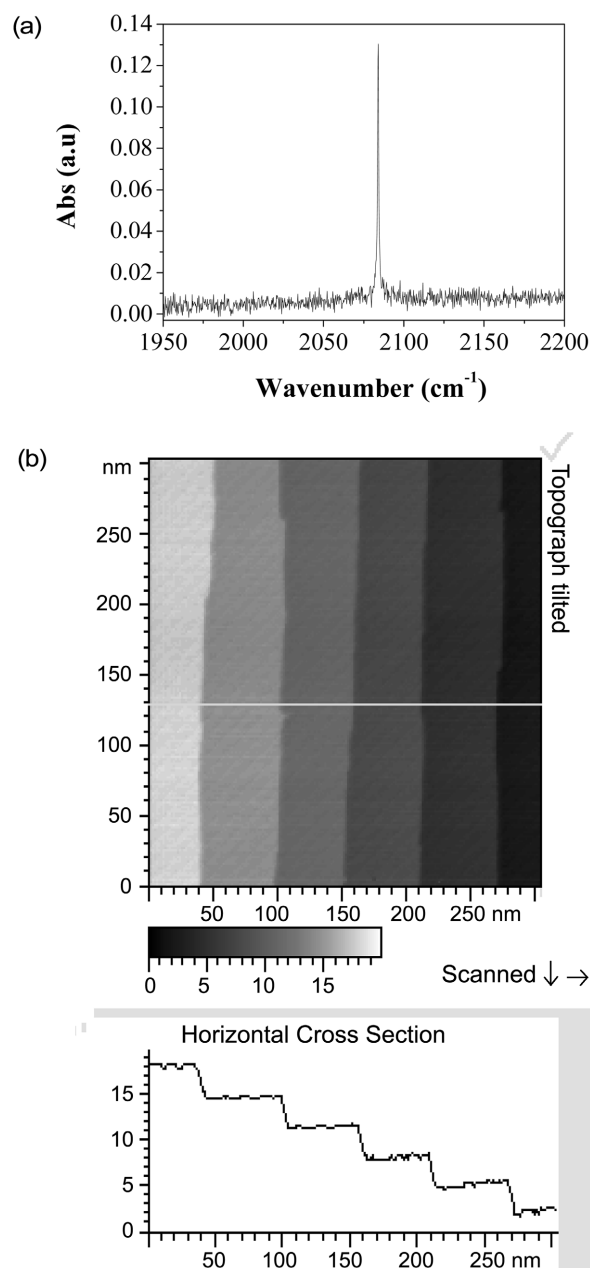


**Figure 1.** (a) P-polarized ATR-FTIR spectrum and (b) STM image (Frame size is  $0.5 \times 0.5 \mu\text{m}^2$ ) of a hydrogen-terminated Si(111) surface after immersing in nitrogen-purged 40% NH<sub>4</sub>F solution for 5 min.

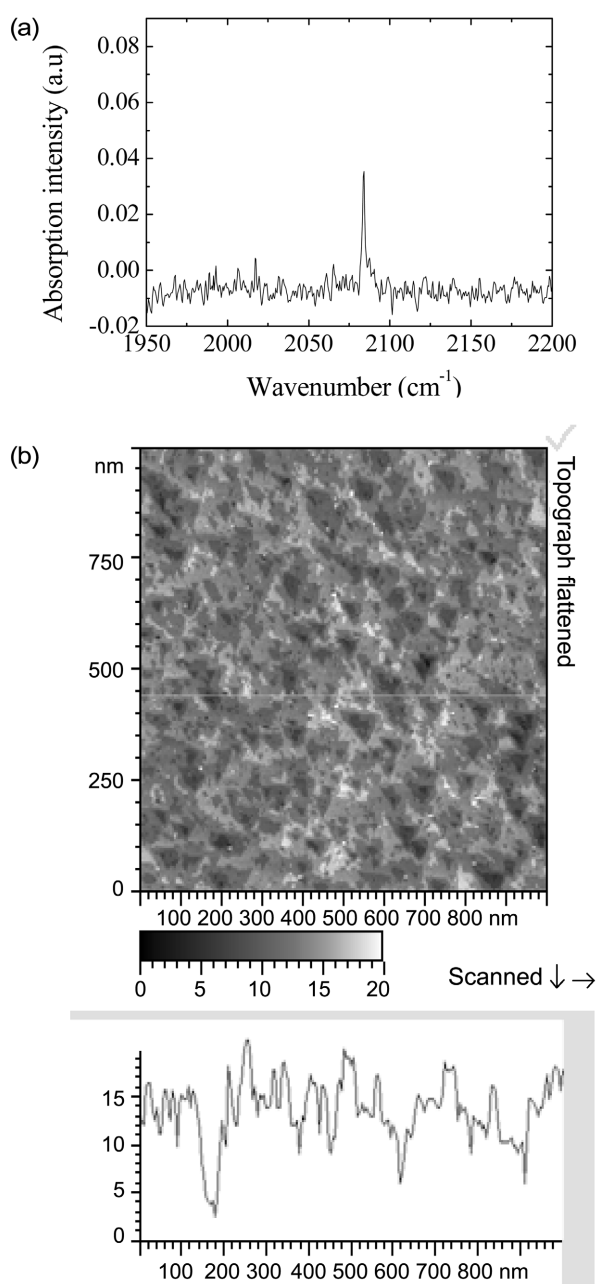


**Figure 2.** (a) P-polarized ATR-FTIR spectrum and (b) STM image (Frame size is  $1 \times 1 \mu\text{m}^2$ ) of a hydrogen-terminated Si(111) surface after immersing in oxygen-saturated 40%  $\text{NH}_4\text{F}$  solution for 5 min.

gas. An ATR-FTIR spectrum and an STM image (Frame size is  $1 \times 1 \mu\text{m}^2$ ) of the hydrogen-terminated Si(111) surface which was prepared in nitrogen-purged 40%  $\text{NH}_4\text{F}$  solution for 5 min followed by immersion in oxygen-saturated 40%  $\text{NH}_4\text{F}$  solution are displayed in Figures 2(a) and 2(b), respectively. The STM image (Fig. 2(b)) had a large number of triangular pits. It was proposed by Chidsey *et al.* that a dissolved oxygen was reduced to superoxide anion radical  $\text{O}_2^-$ , which started to form triangular pits by abstraction of the hydride from a surface silicon atom.<sup>7</sup> Therefore, it is concluded from ATR-FTIR spectrum of Figure 2(a) and from STM image of Figure 2(b) that the

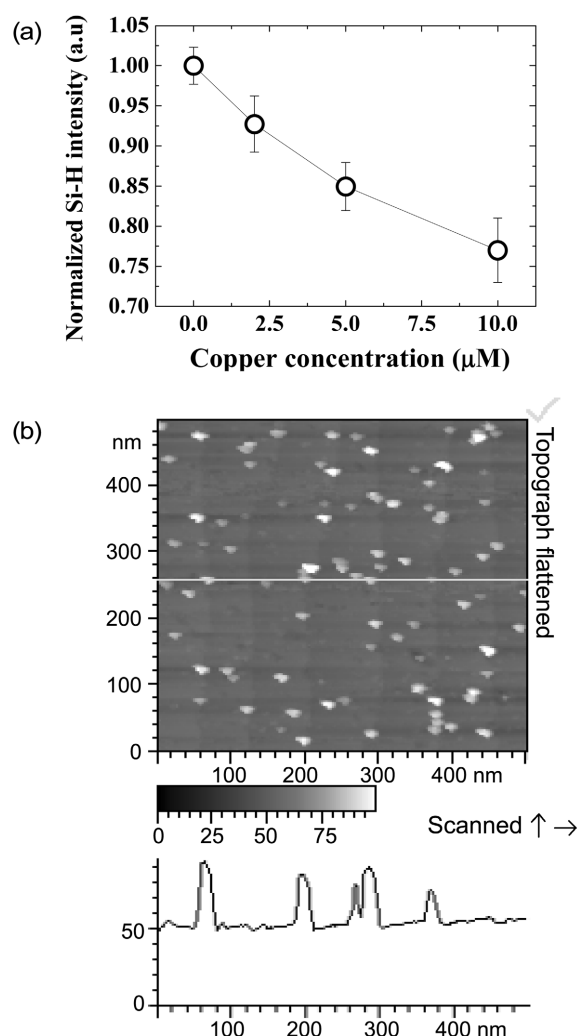


**Figure 3.** (a) Change in normalized hydrogen-terminated Si(111) intensities as a function of Cu(II) concentration of nitrogen-purged 40%  $\text{NH}_4\text{F}$  solution. (b) STM image (Frame size is  $0.5 \times 0.5 \mu\text{m}^2$ ) of a Si(111) surface immersed in nitrogen-purged 40%  $\text{NH}_4\text{F}$  solution containing  $10 \mu\text{M}$  Cu(II) for 5 min.

decrease in the ATR-FTIR intensity of the terminated-monohydride adsorbed on the flat Si(111) surface is directly related to the presence of the triangular pits or the roughened surface, which could originate from the surface hydride abstraction by  $\text{O}_2^-$  produced.

Figure 3(a) shows a change in normalized ATR-FTIR intensities of surface Si-H bonds as a function of Cu(II) concentration. The ATR-FTIR intensity or population of the terminated-H on the Si surface decreased as Cu(II) concentration increased. An STM image (Frame size is  $0.5 \times 0.5 \mu\text{m}^2$ ) of an Si(111) surface immersed in nitrogen-purged 40%  $\text{NH}_4\text{F}$  solution containing  $10 \mu\text{M}$  Cu(II) for 5 min is shown in Figure 3(b). The bright spots formed on the step edge of the terrace surface were the adsorbed Cu islands.<sup>5</sup> The number of monohydrides on an Si terrace decreased as the concentration of Cu(II) increased because the surface hydride abstraction reaction took place between the hydrogen-terminated Si and Cu(II) in solution to give rise to

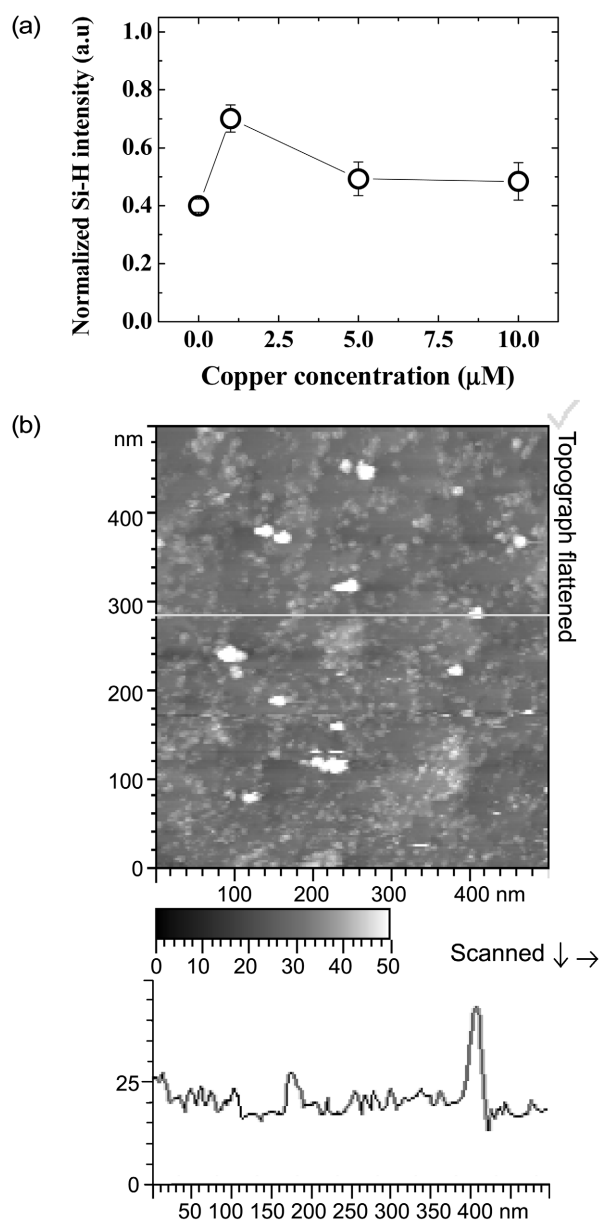


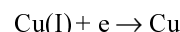
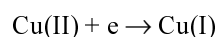
**Figure 4.** (a) Change in normalized hydrogen-terminated Si(111) intensities as a function of Cu(II) concentration of oxygen-saturated 40%  $\text{NH}_4\text{F}$  solution. (b) STM image (Frame size is  $0.5 \times 0.5 \mu\text{m}^2$ ) of a Si(111) surface immersed in oxygen-saturated 40%  $\text{NH}_4\text{F}$  solution containing  $10 \mu\text{M}$  Cu(II) for 5 min.

the roughened silicon surface with the copper nano particles produced at step edges.

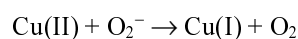
Figure 4(a) shows a change in normalized ATR-FTIR intensities of surface Si-H bonds after immersing the hydrogen-terminated Si(111) in oxygen-purged 40%  $\text{NH}_4\text{F}$  solution containing Cu(II) ions for 5 min. The intensity at  $2084 \text{ cm}^{-1}$  corresponding to hydrogen-terminated Si stretching mode decreased with increasing Cu(II) concentration. The normalized intensities were 0.7-0.5 depending on the concentration of Cu(II) in the ranges of 1-10  $\mu\text{M}$ . However, the intensity of the monohydride adsorbed on the Si(111) surface in 1-10  $\mu\text{M}$  copper-containing, oxygen-saturated

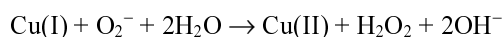
solution was less reduced than that (The normalized intensity was calculated to be 0.4 from the ratio of Figure 2(a) to Figure 1(a)) in Cu(II)-free,  $\text{O}_2$ -saturated solution. Such a decrease in the monohydride intensity on the hydrogen-terminated Si(111) surface in the solution with both Cu and  $\text{O}_2$  present is unable to be explained by the simple summation of reductions on only  $\text{O}_2$ -saturated solution and on only Cu(II)-containing solution. Figure 4(b) shows STM image (Frame size is  $0.5 \times 0.5 \mu\text{m}^2$ ) of an Si(111) surface immersed in oxygen-saturated 40%  $\text{NH}_4\text{F}$  solution containing  $10 \mu\text{M}$  Cu(II) for 5 min. The pits having somewhat round shape were observed over wide surface regions. However, it was clearly discernable that the density of the pits was lower than that appearing in Figure 2(b), which was obtained after immersing in Cu(II)-free oxygen-saturated 40%  $\text{NH}_4\text{F}$  solution for 5 min and that the density of copper nano particles was lower than that in Figure 3(b), in  $\text{O}_2$ -free  $10 \mu\text{M}$  Cu(II). Our STM image is in accord with the previous STM and AFM observations.<sup>7-12</sup>

The intensity of hydrogen-terminated Si(111) in an oxygen-dissolved solution decreased by 60% compared with the hydrogen-terminated Si surface as shown in Figures 1(a) and 2(a). However, in the case of  $\text{O}_2$ -saturated  $\text{NH}_4\text{F}$  solution with a Cu(II) concentration of 1-10  $\mu\text{M}$  (Fig. 4(a)) the ATR-FTIR intensity of the monohydride on the sample was reduced by 30-50% as compared with that on the sample of Figure 1(a). Nitrogen-purged 40%  $\text{NH}_4\text{F}$  solution with 1-10  $\mu\text{M}$  Cu(II) ions made the monohydride of the hydrogen-terminated Si(111) sample reduced to 77-93% as displayed in Figure 3(a). On the other hand, it was expected from the simple summation of the two independent hydride abstraction reactions by oxygen and Cu(II) reductions that the intensity of the monohydride reduced to 17-33% in  $\text{O}_2$ -saturated  $\text{NH}_4\text{F}$  solution with 1-10  $\mu\text{M}$  Cu(II) ions, which was significantly smaller than 50-70% (Fig. 4(a)). A hydrogen-terminated Si(111) surface was studied by means of STM after immersing into air-saturated  $\text{NH}_4\text{F}$  solution containing Cu(II) ions.<sup>9</sup> The STM image has less triangular pits, induced by superoxide anion radical  $\text{O}_2^-$ , than that of the hydrogen-terminated Si(111) surface immersed in Cu(II)-free, oxygen-saturated 40%  $\text{NH}_4\text{F}$  solution. The reason for this is that copper ions act as catalyst for the disproportionation of the superoxide anion radicals. In the presence of copper ions, the Cu species started to be nucleated over the hydrogen-terminated Si surface through the successive reactions<sup>13,14</sup> of



On the other hand, in the presence of dissolved oxygen, the growth of the Cu islands was slowed down by superoxide ion produced. The reactions between the Cu(II) and superoxide ion were reported from radioysis as shown below.<sup>13,14</sup>





Therefore the presence of the copper ions causes to decrease the concentration of superoxide ion. Similarly, less decrease in the ATR-FTIR intensity of the hydrogen-terminated Si(111) surface in the Cu(II)-containing, oxygen-dissolved solution can be compromised with the additional, other than surface charge transfers and hydride abstractions, pathways of the disproportionation of the formed superoxide anion radicals by Cu(II) ions. Firstly, the reaction of Cu(II) ions and  $\text{O}_2^-$ , which was produced from one-electron transfer reaction from the hydrogenated Si(111) to molecular oxygen, gave rise to Cu(I) ions and  $\text{O}_2$ . Finally, Cu(I) ions were oxidized to the initial Cu(II) ions and  $\text{O}_2^-$  were changed to  $\text{H}_2\text{O}_2$  and  $2\text{OH}^-$ . As a result, the ATR-FTIR intensity of the monohydride on the surface after immersing in the  $\text{O}_2$ -saturated solution with Cu(II) ions remained less reduced than that in the Cu(II)-free,  $\text{O}_2$ -saturated solution. Thus oxygen and Cu(II), two common impurities in wet process, react with hydrogen-terminated Si(111) surface to result in roughened Si(111) surface and the reactions between superoxide anion radicals and copper ions occurs concurrently in etching solutions.

In conclusion, the hydrogen-terminated Si(111) surface and its change after immersion into the three different solutions of Cu(II)-free  $\text{O}_2$ -saturated  $\text{NH}_4\text{F}$  solution,  $\text{O}_2$ -free Cu(II)-containing  $\text{NH}_4\text{F}$  solution, and Cu(II)-containing  $\text{O}_2$ -saturated  $\text{NH}_4\text{F}$  solution were investigated by using ATR-FTIR together with STM. The ATR-FTIR intensity of the monohydride on the Si(111) surface in the Cu(II)-containing, oxygen-dissolved solution was less reduced than what was expected from the summation of the two independent hydride abstraction reactions by Cu(II) and oxygen reductions in  $\text{NH}_4\text{F}$  solution. The observation was explained based on the disproportionation of the superoxide anion radicals by copper ions, in addition to the surface reactions between hydrogenated-Si(111) and oxygen or Cu(II) ions.

### Experimental Section

The apparatus and the sample preparation procedure have been described elsewhere.<sup>5</sup> The parallelogram ATR prism ( $36 \times 20 \times 0.5$  mm,  $45^\circ$  bevel angle) was prepared from phosphorous doped n-type Si(111) wafers ( $1.0\text{--}10 \ \Omega\text{-cm}$ ),

which were polished on both sides for the ATR-FTIR measurements in a multiple internal reflection geometry. A hydrogen-terminated Si(111) surface was prepared by immersing the Si(111) wafer in nitrogen-purged 40%  $\text{NH}_4\text{F}$  solution. ATR-FTIR measurement was performed using a Bio-Rad Excaliber<sup>TM</sup> spectrometer equipped with HgCdTe (MCT) detector cooled with liquid nitrogen. An  $\text{N}_2$  gas was continuously introduced into the FTIR chamber. The ATR-FTIR spectra were recorded in *p*-polarization to compare the effects of Cu(II) ions and dissolved oxygen on the surface processes of the hydrogen-terminated Si(111) surface. The experiment for STM was carried out using a PicoSPM (Molecular Imaging Corp.). The samples for STM measurement were  $1 \times 1 \text{ cm}^2$  and was also investigated under the same condition as the ATR-FTIR.

**Acknowledgements.** This work was supported by Korea Research Foundation (KRF-2002-070-C00050). Helpful discussions with Prof. M. Matsumura are gratefully acknowledged.

### References

1. See for example, *Ultran Clean Processing of Silicon Surfaces VII*; Mertens, P.; Meuris, M.; Heyns, M., Eds.; Solid State Phen.: 2005; Vol. 103.
2. Sawada, Y.; Tsujino, K.; Matsumura, M. *Abstracts of the 208<sup>th</sup> ECS Meeting*; **2005**, 2005-2, 156.
3. Higashi, G. S.; Chabal, Y. J.; Trucks, G. W.; Raghavachari, K. *Appl. Phys. Lett.* **1990**, *56*, 656.
4. Watanabe, S.; Nakamura, N.; Ito, T. *Appl. Phys. Lett.* **1991**, *59*, 1458.
5. Lee, I.-C.; Bae, S.-E.; Song, M.-B.; Lee, J.-S.; Paek, S.-H.; Lee, C.-W. *J. Bull. Korean Chem. Soc.* **2004**, *25*, 167.
6. Ye, S.; Ishihara, T.; Uosaki, K. *J. Electrochem. Soc.* **2001**, *148*, C421.
7. Wade, C. P.; Chidsey, C. E. D. *Appl. Phys. Lett.* **1997**, *71*, 1697.
8. Fukidome, H.; Matsumura, M. *Appl. Surf. Sci.* **1998**, *130*, 146.
9. Homma, T.; Wade, C. P.; Chidsey, C. E. D. *J. Phys. Chem.* **1998**, *B102*, 7919.
10. Homma, T.; Tsukano, J.; Osaka, T. *Electrochem. Soc. Proc.* **1999**, *99-34*, 95.
11. Allongue, P.; de Villeneuve, C. H.; Morin, S.; Boukherroub, R.; Wayner, D. D. M. *Electrochim. Acta* **2000**, *45*, 4591.
12. Chemla, M.; Homma, T.; Bertabna, V.; Erre, R.; Kubo, N.; Osaka, T. *J. Electroanal. Chem.* **2003**, *559*, 111.
13. Von Piechowski, M.; Nauser, T.; Hoigne, J.; Buhler, R. E. *Ber. Bunsen-Ges. Phys. Chem.* **1993**, *97*, 762.
14. Ravani, J.; Klug-Roth, D.; Lilie, J. *J. Phys. Chem.* **1973**, *77*, 1169.